

On The Optimal Number of Reflecting Elements for Reconfigurable Intelligent Surfaces

Alessio Zappone, *Senior Member IEEE*, Marco Di Renzo, *Fellow IEEE*, Xiaojun Xi, *Student Member, IEEE*, Merouane Debbah, *Fellow IEEE*

Abstract—This work considers a point-to-point link where a reconfigurable intelligent surface assists the communication between transmitter and receiver. The system rate, energy efficiency, and their trade-off are optimized with respect to the number of individually tunable elements of the intelligent surface. The resource allocation accounts for the communication phase and for the overhead due to channel estimation and to reporting the optimized resource allocation to the intelligent surface. Numerical results confirm the optimality of the proposed methods and show the potential gains of reconfigurable intelligent surfaces.

I. INTRODUCTION

Recently, the concept of smart radio environment has emerged as a candidate architecture for future 6G networks [1], [2], [3], [4], [5], [6], wherein reconfigurable intelligent surfaces (RISs) are used to coat environmental objects that are present in the propagation environment. An RIS is a planar structure made of several individually tunable elements, called meta-atoms or passive scatterers, that can be programmed and appropriately reconfigured to control the phase of the incoming electromagnetic signal, by reflecting or refracting it towards specified locations [1]. In [7] and [8] the signal-to-noise ratio (SNR) scaling law of RIS-aided transmission is characterized, and the impact of hardware impairments are analyzed, respectively. Experimental testbeds have confirmed the potential gains of RISs [9], [10], [11], [12].

In the context of radio resource allocation, several works have appeared. In [13], the rate and energy efficiency (EE) of an RIS-based multiple input single output (MISO) downlink system are optimized by means of alternating optimization, fractional programming, and sequential optimization. A similar system setup is addressed in [14], and the problem of power minimization subject to minimum rate constraints is tackled by alternating optimization. In [15] and [16], sum-rate maximization in a MISO downlink system with orthogonal frequency division multiplexing is studied by optimizing the transmit beamformer and the RIS phase shifts with the aid of alternating optimization. An RIS with discrete phase shifts is considered in [17], where sum-rate maximization in a multi-user MISO system is addressed. In [18], a multi-user MISO channel is considered, in which an RIS is used to perform over-the-air computations. Alternating optimization and difference convex programming are used for system optimization. In [19],

multiple RISs are used in a massive multiple-input multiple-output (MIMO) setup, and the problem of maximizing the minimum of the users' signal-to-interference-plus-noise-ratio with respect to the transmit precoder and the RISs phase shifts is considered. In [20], the problem of power control for physical-layer broadcasting under quality of service constraints for the mobile users is addressed. The downlink of a MIMO multi-cell system is considered in [21], wherein the problem of weighted sum-rate maximization is tackled by alternatively optimizing the base station beamformer and the RIS phase shifts. An RIS-based MISO millimeter-wave system is studied in [22], wherein the transmit beamforming and the phase shifts of multiple RISs are optimized. In [23], channel estimation and sum-rate maximization are performed for a single-user uplink RIS-based system, by considering an RIS with discrete phase shifts. In [24], the sum-rate of a MIMO RIS-based system employing simultaneous information and power transfer is maximized with respect to the transmitter beamforming and the RIS phase shifts. Power control for physical layer broadcasting in an RIS-based network is investigated in [25]. Rate maximization for RIS-based indoor millimeter-waves communications is addressed in [26] by adjusting the RIS and the transmitter phase shifts.

The above literature survey shows that most works focus on how to maximize the rate of RIS-based systems with respect to the transmit power/beamforming and to the RIS phase shifts, whereas the number of tunable elements at the RIS is not optimized. Moreover, previous works consider only the data transmission phase, while neglecting the overhead for channel estimation and reporting the optimized configuration to the RIS. In contrast to these research works, this paper addresses the problem of jointly optimizing the RIS phase shifts and the number of tunable elements to be activated at the RIS, in order to optimize the rate, the EE and their trade-off. Notably, this is performed based on the model recently proposed in [27], which quantifies the impact of channel estimation and resource allocation feedback on the rate and EE of RIS-based systems.

The rest of the paper is organized as follows. Section II describes the system model, Sections III, IV, and V develop the proposed algorithm for the optimization of the rate, EE, and their trade-off, respectively. Section VI numerically analyzes the proposed algorithms, while concluding remarks are given in Section VII.

II. SYSTEM MODEL AND PROBLEM STATEMENT

We consider a point-to-point system wherein a single-antenna transmitter and receiver communicate through an RIS

A. Zappone is with the University of Cassino and Southern Lazio, Cassino, Italy (alessio.zappone@unicas.it). M. Di Renzo and X. Xi are with the Université Paris-Saclay, CNRS and CentraleSupélec, Laboratoire des Signaux et Systèmes, 91192 Gif-sur-Yvette, France (marco.direnzo@centralesupelec.fr), M. Debbah is with Huawei France R&D, Boulogne-Billancourt, France (merouane.debbah@huawei.com).

equipped with N individually tunable elements. This scenario models, for example, a device-to-device communication link, or a cellular network in which the base stations employ antenna selection to serve each user by a different antenna, and multi-user interference is suppressed by orthogonal frequency division multiple access or any other orthogonal signaling technique. Also, numerical results in [27] have shown that RISs are especially useful when few antennas are employed, since a proper RIS design can compensate for the lack of multiple transmit and/or receive antennas, without suffering a large overhead for channel estimation and feedback.

We assume that the direct path between transmitter and receiver is not available, and denote by $\mathbf{h} = \{h_n\}_{n=1}^N$ and $\mathbf{g} = \{g_n\}_{n=1}^N$ the fast-fading vector channels from the transmitter to the RIS and from the RIS to the receiver, and by δ the overall propagation path-loss. Before data communication can take place, the channels \mathbf{h} and \mathbf{g} must be estimated and the RIS configuration must be optimized and deployed at the RIS. Channel estimation and RIS optimization can take place at either the transmitter or the receiver through traditional pilot signaling techniques, while the optimized RIS configuration is implemented thanks to an RIS controller with minimal signal processing, transmission/reception, and power storage capabilities. It should be stressed that the presence of the controller is essential in order for the RIS to be dynamically reconfigurable in response to changes of the propagation channels [1, Fig. 4]. On the other hand, sending the control signal to the RIS introduces a non-negligible overhead to the communication phase, especially for large N . Denoting by T the total duration of the time slot comprising the channel estimation phase of duration T_E , the control feedback phase of duration T_F , and the data communication phase of duration $T - T_E - T_F$, and defining $\beta = p\delta/(BN_0)$, with B the communication bandwidth, N_0 the receive power spectral density, and p the transmit power, the system rate and EE are expressed as

$$R(N) = \left(1 - \frac{T_E + T_F}{T}\right) B \log(1 + \beta |\mathbf{g}^H \mathbf{\Phi} \mathbf{h}|^2) \quad (1)$$

$$\text{EE}(N) = R(N)/P_{tot} \quad (2)$$

wherein $\mathbf{\Phi} = \text{diag}(e^{j\phi_1}, \dots, e^{j\phi_N})$ is the RIS phase matrix and P_{tot} is the total power consumption in the whole time-frame T . Following the model developed in [27], we have $T_E = T_0(N+1)$, with T_0 the duration of each pilot tone, and

$$T_F = \frac{Nb_F}{B_F \log(1 + p_F |h_F|^2 / (N_0 B_F))} \quad (3)$$

$$P_{tot} = P_E + (1 - T_E/T)\mu p + T_F/T(\mu_F p_F - \mu p) + NP_{c,n} + P_{c,0},$$

since a power p is used for $T - T_E - T_F$ seconds, with transmit amplifier efficiency $1/\mu$, a power p_F is used for T_F seconds, with transmit amplifier efficiency $1/\mu_F$, while hardware static power is consumed during the whole interval T , where $P_{c,n}$ is the hardware power required for each RIS element, $P_{c,0}$ is the hardware power for all other system components, and $P_E = T_E P_0/T$ is the power consumption during the channel estimation phase, with P_0 the power of each pilot tone.

The aim of this work is to optimize the RIS phase shift matrix $\mathbf{\Phi}$ and the number of tunable elements N at the RIS,

in order to optimize the system rate and EE in (1), and their trade-off. Note that the approach in this work differs from robust resource allocation methods which assume imperfect channel state information [28], [29], [30]. Indeed, we assume that reliable channel estimation is performed and the resulting overhead is appropriately accounted for in our system model.

A. Optimization of $\mathbf{\Phi}$ And Upper-Bound of N

Since $\mathbf{\Phi}$ does not affect the power consumption P_{tot} , the optimal $\mathbf{\Phi}$ for both the rate and the EE is obtained by maximizing the term $|\mathbf{g}^H \mathbf{\Phi} \mathbf{h}|^2$. It is easy to see that this is accomplished by setting $\phi_n = \angle g_n^* h_n$ for any n . With this choice, the received power at the destination is $p\delta \left(\sum_{n=1}^N \alpha_n\right)^2$, with $\alpha_n = |h_n g_n|$. On the other hand, since the received power can not be larger than the transmit power, it must hold that $\delta \left(\sum_{n=1}^N \alpha_n\right)^2 \leq 1$. Defining $\alpha_{max} = \max_n \alpha_n$, a sufficient condition for this to hold is $N\alpha_{max}\sqrt{\delta} \leq 1$, which sets an upper-bound on the maximum number of elements that can be placed on the RIS in order for the considered path-loss model to be physically meaningful. In addition, in order to prove the mathematical results to follow, we assume $\beta\alpha_{max}^2 \geq 1$. This appears realistic, since $\beta\alpha_{max}^2$ is the receive SNR over the reflection path with the largest gain. Moreover, since $N\alpha_{max}\sqrt{\delta} \leq 1$, in order to enforce $\beta\alpha_{max}^2 \geq 1$ we must have $N^2 \leq \beta/\delta$, which finally allows us to bound the maximum number N_{max} of elements at the RIS as

$$N_{max} \leq \min \left\{ (\alpha_{max}\sqrt{\delta})^{-1}, \sqrt{\beta/\delta} \right\}. \quad (4)$$

III. RATE OPTIMIZATION

Plugging the optimal $\mathbf{\Phi}$, the rate maximization problem is

$$\max_{1 \leq N \leq \min\{N_{max}, \lfloor c/d \rfloor\}} (c - dN) B \log \left(1 + \beta \left(\sum_{n=1}^N \alpha_n \right)^2 \right) \quad (5)$$

with $c = 1 - \frac{T_0}{T}$, $d = \frac{T_0}{T} + \frac{b_F}{TB_F \log(1 + \frac{p_F |h_F|^2}{B_F N_0})}$, and where, without loss of generality, we consider that the coefficients α_n are arranged in decreasing order of magnitude, i.e. $\alpha_n \geq \alpha_{n+1}$ for all $n = 1, \dots, \min\{N_{max}, \lfloor \frac{c}{d} \rfloor\}$, which also means that $\alpha_{max} = \alpha_1$. The constraint in (5) ensures that the sum of the durations of the channel estimation and feedback phases is shorter than the total length of the frame, and that N is smaller than its maximum feasible number N_{max} . The challenge in solving (5) lies in the fact that the first factor of the objective decreases with N , while the second factor increases with N , which makes it difficult to determine the behavior of the rate R as a function of the discrete variable N . In order to globally solve (5), the following result is instrumental.

Proposition 1: $R(N)$ in (5) is a unimodal function, i.e. it is either increasing with N or, if there exists an \bar{N} such that $R(\bar{N}) \geq R(\bar{N} + 1)$, $R(N)$ is decreasing for $N \geq \bar{N}$.

Proof: If \bar{N} does not exist, the rate is increasing with N . If \bar{N} exists, then defining $f(N) = B \log \left(1 + \beta \left(\sum_{n=1}^N \alpha_n \right)^2 \right)$, the condition $R(\bar{N}) \geq R(\bar{N} + 1)$ is equivalent to

$$(c - d\bar{N})(f(\bar{N} + 1) - f(\bar{N})) \leq d f(\bar{N} + 1). \quad (6)$$

Thus, the result holds if we can show that (6) implies that $R(\bar{N} + 1) \geq R(\bar{N} + 2)$, i.e.

$$(c - d(\bar{N} + 1))(f(\bar{N} + 2) - f(\bar{N} + 1)) \leq d f(\bar{N} + 2). \quad (7)$$

At this point, let us show that, for any N , it holds

$$f(N + 1) - f(N) \geq f(N + 2) - f(N + 1). \quad (8)$$

To see this, expanding the square in $f(N + 1)$ leads to

$$\begin{aligned} f(N + 1) - f(N) &= \\ B \log \left(1 + \frac{\beta \left(\left(\sum_{n=1}^N \alpha_n \right)^2 + \alpha_{N+1}^2 + 2\alpha_{N+1} \sum_{n=1}^N \alpha_n \right)}{1 + \beta \left(\sum_{n=1}^N \alpha_n \right)^2} \right) &= \\ B \log \left(1 + \frac{\beta \alpha_{N+1} \left(\alpha_{N+1} + 2 \sum_{n=1}^N \alpha_n \right)}{1 + \beta \left(\sum_{n=1}^N \alpha_n \right)^2} \right) & \end{aligned} \quad (9)$$

Similarly, it holds

$$f(N + 2) - f(N + 1) = B \log \left(1 + \frac{\beta \alpha_{N+2} \left(\alpha_{N+2} + 2 \sum_{n=1}^{N+1} \alpha_n \right)}{1 + \beta \left(\sum_{n=1}^{N+1} \alpha_n \right)^2} \right).$$

Then, the condition in (8) becomes

$$\begin{aligned} \frac{\alpha_{N+1}^2}{1 + \beta \left(\sum_{n=1}^N \alpha_n \right)^2} + \frac{2\alpha_{N+1} \sum_{n=1}^N \alpha_n}{1 + \beta \left(\sum_{n=1}^N \alpha_n \right)^2} &\geq \\ \frac{\alpha_{N+2}^2}{1 + \beta \left(\sum_{n=1}^{N+1} \alpha_n \right)^2} + \frac{2\alpha_{N+2} \sum_{n=1}^{N+1} \alpha_n}{1 + \beta \left(\sum_{n=1}^{N+1} \alpha_n \right)^2}. & \end{aligned} \quad (10)$$

Since $\alpha_n \geq \alpha_{n+1}$ for any $n = 1, \dots, N$, the first summand at the left-hand-side of (10) is larger than the first summand at the right-hand-side. Then, a sufficient condition for (10) to hold is

$$\frac{\sum_{n=1}^N \alpha_n}{1 + \beta \left(\sum_{n=1}^N \alpha_n \right)^2} \geq \frac{\sum_{n=1}^{N+1} \alpha_n}{1 + \beta \left(\sum_{n=1}^{N+1} \alpha_n \right)^2}. \quad (11)$$

Defining $z = \sum_{n=1}^N \alpha_n$, it can be seen that (11) is equivalent to showing that the function $g(z) = \frac{z}{1 + \beta z^2}$ is decreasing. Computing the first-order derivative of $g(z)$, and setting it to be non-positive, yields $\beta \alpha_1 \geq 1$, which holds on the feasible set of (5). Finally, exploiting (6), and observing that $f(N)$ is increasing in N since each α_n is positive, it follows that

$$\begin{aligned} (c - d(\bar{N} + 1))(f(\bar{N} + 2) - f(\bar{N} + 1)) &\leq \\ (c - d\bar{N})(f(\bar{N} + 1) - f(\bar{N})) &\leq \\ d f(\bar{N} + 1) &\leq d f(\bar{N} + 2), \end{aligned} \quad (12)$$

and hence the proof follows. \blacksquare

Equipped with this result, Problem (5) can be solved by a greedy approach in which the tunable elements of the RIS are activated one at a time, following the decreasing order of magnitude of the coefficients $\{\alpha_n\}_n$, until a decrease in $R(N)$ is observed, or N reaches its maximum allowed number. The procedure is stated in Algorithm 1, with $A(N) = R(N)$.

Algorithm 1 Optimization of N for rate maximization

```

 $\bar{N} = 1$ ;  $A_0 = 0$ ;  $A_1 = A(\bar{N})$ ;
while  $A_n \geq A_{n-1}$  and  $N \leq \min \{N_{max}, \lfloor \frac{c}{d} \rfloor\}$  do
   $N = N + 1$ ;
   $A_n = A(N)$ ;
end while

```

IV. ENERGY EFFICIENCY OPTIMIZATION

Defining $\gamma = P_{c,0} + P_0 \frac{T_0}{T} + \mu p c$ and $\psi = (P_0 - \mu p - 1) \frac{T_0}{T} + d + P_{c,n}$, the EE maximization problem is stated as

$$\max_N \frac{(c - dN)f(N)}{\gamma + \psi N} \quad (13a)$$

$$\text{s.t. } 1 \leq N \leq \min \{N_{max}, \lfloor c/d \rfloor\}. \quad (13b)$$

Proposition 2 shows that the EE is unimodal, and thus (13a) can be globally solved by Algorithm 1 with $A(N) = \text{EE}(N)$.

Proposition 2: $\text{EE}(N)$ in (13a) is a unimodal function, i.e. it is either increasing with N or, if there exists an \bar{N} such that $\text{EE}(\bar{N}) \geq \text{EE}(\bar{N} + 1)$, $\text{EE}(N)$ is decreasing for $N \geq \bar{N}$.

Proof: Proceeding like in the proof of Proposition 1, if \bar{N} does not exist, then $\text{EE}(N)$ is increasing with N . Instead, if \bar{N} exists, the result follows if we can prove that $\text{EE}(\bar{N}) \geq \text{EE}(\bar{N} + 1)$ implies that $\text{EE}(\bar{N} + 1) \geq \text{EE}(\bar{N} + 2)$. First of all, let us observe that if \bar{N} is such that $R(\bar{N}) \geq R(\bar{N} + 1)$, then we already know from Proposition 1 that \bar{N} falls in the range in which the rate function $R(N)$ is decreasing. This implies that the EE is decreasing for any $N \geq \bar{N}$, since increasing N yields a lower numerator and a larger denominator. As a result, the non-trivial case to be considered is when \bar{N} belongs to the range in which the rate is still increasing, i.e. the first decrease in the EE happens when the rate function is still increasing with N . Thus, without loss of generality, in the rest of this proof we assume $R(\bar{N} + 2) > R(\bar{N} + 1) > R(\bar{N})$. Next, let us observe that $\text{EE}(\bar{N}) \geq \text{EE}(\bar{N} + 1)$ is equivalent to

$$\bar{N} \leq -\frac{\gamma}{\psi} + \frac{R(\bar{N})}{R(\bar{N} + 1) - R(\bar{N})}. \quad (14)$$

Similarly, $\text{EE}(\bar{N} + 1) \geq \text{EE}(\bar{N} + 2)$ is equivalent to

$$\bar{N} \leq -\frac{\gamma}{\psi} - 1 + \frac{R(\bar{N} + 1)}{R(\bar{N} + 2) - R(\bar{N} + 1)}. \quad (15)$$

At this point, we note that (14) can be written as

$$\bar{N} \leq -\frac{\gamma}{\psi} - 1 + \frac{R(\bar{N} + 1)}{R(\bar{N} + 1) - R(\bar{N})}, \quad (16)$$

which implies (15) if we can show that $R(\bar{N} + 2) - R(\bar{N} + 1) \leq R(\bar{N} + 1) - R(\bar{N})$. To show this, we observe that we have

$$\begin{aligned} R(\bar{N} + 2) - R(\bar{N} + 1) &= \\ &= (c - d(\bar{N} + 1)) (f(\bar{N} + 2) - f(\bar{N} + 1)) - df(\bar{N} + 2) \\ &\leq (c - d(\bar{N} + 1)) (f(\bar{N} + 2) - f(\bar{N} + 1)) - df(\bar{N}) \\ &\leq (c - d(\bar{N} + 1)) (f(\bar{N} + 1) - f(\bar{N})) - df(\bar{N}) \\ &= R(\bar{N} + 1) - R(\bar{N}), \end{aligned} \quad (17)$$

where the two equalities follow recalling that $R(N) = (c - dN)f(N)$, while the two inequalities follow since $f(N)$ is

non-negative, increasing, and such that $f(N + 1) - f(N) \geq f(N + 2) - f(N + 1)$, as proved in Proposition 1. ■

V. RATE-EE MAXIMIZATION

Rate-EE maximization is cast as the bi-objective problem

$$\max_N \{R(N), EE(N)\}, \text{ s.t. } 1 \leq N \leq \min\{N_{max}, \lfloor c/d \rfloor\} \quad (18)$$

By virtue of [31, Th. 3.4.5], all Pareto-optimal points of (18) can be obtained by solving

$$\max_N \min\{w(R(N) - R_{opt}), (1-w)(EE(N) - EE_{opt})\} \quad (19a)$$

$$\text{s.t. } 1 \leq N \leq \min\left\{N_{max}, \left\lfloor \frac{c}{d} \right\rfloor\right\} \quad (19b)$$

for $w \in (0, 1)$, with R_{opt} and EE_{opt} the individual maximizers of $R(N)$ and $EE(N)$, that as derived in Sections III and IV. The following proposition shows that $G(N) = \min\{w(R(N) - R_{opt}), (1-w)(EE(N) - EE_{opt})\}$ is unimodal, and thus Problem (19a) can be solved by Algorithm 1 with $A(N) = G(N)$.

Proposition 3: $G(N)$ is a unimodal function, i.e. it is either increasing with N , or, if there exists \bar{N} such that $G(\bar{N}) \geq G(\bar{N} + 1)$, $G(N)$ is decreasing for $N \geq \bar{N}$.

Proof: Propositions 1 and 2 ensure that $R(N)$ and $EE(N)$ are unimodal functions, which implies that $G_1 = w(R(N) - R_{opt})$ and $G_2 = (1-w)(EE(N) - EE_{opt})$ are unimodal, too.

Let us consider first that both $G_1(N)$ and $G_2(N)$ have a finite maximizer, which we denote by N_1 and N_2 , respectively. Without loss of generality, let us assume that $N_1 \leq N_2$. Then, $G(N)$ is increasing for $N \leq N_1$ and decreasing for $N \geq N_2$. As for the range $N_1 < N < N_2$, let us consider two cases:

(a) If $G_1(N_1) \leq G_2(N_1)$, then, $G(N) = G_1(N)$ for $N_1 < N < N_2$, because in this range G_2 is increasing while G_1 is decreasing. As a result, $G(N)$ is increasing for $N \leq N_1$ and decreasing for $N > N_1$ and we have $\bar{N} = N_1$.

(b) If $G_1(N_1) > G_2(N_1)$, two cases can be considered: if $G_1(N) \geq G_2(N)$ for $N_1 \leq N \leq N_2$, then $G(N) = G_2(N)$ for $N_1 \leq N \leq N_2$ and the thesis holds with $\bar{N} = N_2$; if instead $G_1(N) \not\geq G_2(N)$ for $N_1 \leq N \leq N_2$, then we can define N_3 as the smallest number such that $N_1 < N_3 \leq N_2$ and $G_1(N_3) \leq G_2(N_3)$. Thus, $G(N) = G_2(N)$ for $N_1 \leq N < N_3$, while $G(N) = G_1(N)$ for $N_3 \leq N \leq N_2$. Then, it follows that $G(N)$ is increasing for $N < N_3$ and decreasing for $N \geq N_3$, and the thesis follows with $\bar{N} = N_3$.

Finally, we observe that the reasoning above includes as special cases the situations in which either G_1 or G_2 is monotonically increasing for all N , while in the case in which both G_1 and G_2 are monotonically increasing $G(N)$ is monotonically increasing and \bar{N} does not exist. ■

VI. NUMERICAL RESULTS

In our numerical simulation we set $P_F = 30$ dBm, $B = 5$ MHz, $B_F = 1$ MHz, $\delta = 110$ dB, $N_0 = -174$ dBm/Hz, $\mu = \mu_F = 1$, $P_{c,0} = 45$ dBm, $P_{c,n} = 10$ dBm, $b_F = 16$, $T_0 = 0.5$ ms, $P_0 = 10$ dBm. Moreover, $h_n \sim \mathcal{CN}(v_h, 1)$ and $g_n \sim \mathcal{CN}(v_g, 1)$. Thus, $|h_n|$ and $|g_n|$ are Rice distributed, where v_h and v_g are chosen so that the power of the line-of-sight path is four times larger than the power of all other paths. A similar model is used for the feedback channel h_F . Also,

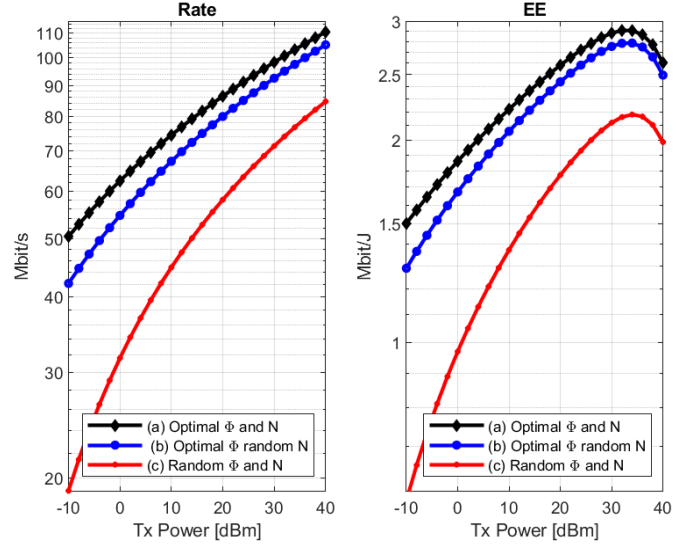


Fig. 1: Rate (left) and EE (right) versus P for: (a) Optimal N and Φ ; (b) Random N and optimal Φ ; (c) Random N and Φ .

	0 dBm	10 dBm	20 dBm	30 dBm	40 dBm
N_R^*	198.89	197.32	193.38	184.74	172.04
N_{EE}^*	187.05	167.29	147.01	133.92	145.99

TABLE I: Network parameters

$N_{max} = 200$ and all presented results have been averaged over 10^4 independent realizations of the channel vectors \mathbf{h} and \mathbf{g} .

Fig. 1 shows the rate and EE versus the transmit power P achieved by the following schemes:

- Optimization of N by Algorithm 1 and optimization of Φ as described in Section II-A.
- Random selection of N in the range $[1, \min\{N_{max}, c/d\}]$ and optimization of Φ as described in Section II-A.
- Random selection of N in the range $[1, \min\{N_{max}, c/d\}]$ and random selection of ϕ_n in $[0, 2\pi]$ for all $n = 1, \dots, N$. Since no configuration of the RIS phase shifts is required for this scheme, we set $T_F = 0$ and $T_E = T_0$ in this case.

The results show that accounting, at the design stage, for the overhead due to channel estimation and optimal RIS configuration outperforms random resource allocation. In particular, the proposed Scheme (a) grants a large gain compared to Scheme (c) which randomly selects both N and Φ , despite the fact that no overhead is required in this case for reporting the resource allocation at the RIS.

Table I reports the rate maximizer N_R^* and the EE maximizer N_{EE}^* versus P corresponding to the performance of Scheme (a) in Fig. 1. The results confirm that both the rate and the EE have a finite maximizer with N .

Finally Fig. 2 shows the Rate-EE Pareto-frontier of the considered RIS-based system for $P = 20$ dBm, $P = 30$ dBm, $P = 40$ dBm. For each value of P the cases $P_{c,n} = 10$ dBm and $P_{c,n} = 15$ dBm are shown. As expected, a higher $P_{c,n}$ yields a wider Pareto-region, because the higher $P_{c,n}$ is, the more the rate and the EE are contrasting objectives.

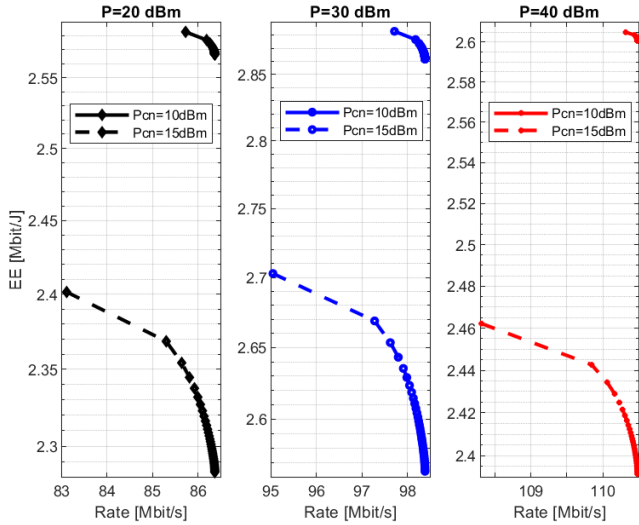


Fig. 2: Rate-EE Pareto region for $P = 20$ dBm (left), 30 dBm (middle), 40 dBm (right), with $P_{c,n} = 10$ dBm and 15 dBm

VII. CONCLUSIONS

This work has optimized the number of tunable elements to be activated on a RIS, by accounting at the design stage for the overhead due to channel estimation and RIS configuration. Globally optimal and low-complexity algorithms are derived for the optimization of the rate, the EE, and their trade-off. Numerical results have confirmed that overhead-aware resource allocation may significantly outperform sub-optimal methods, such as random RIS configuration.

REFERENCES

- [1] M. Di Renzo, A. Zappone, M. Debbah, M. Alouini, C. Yuen, J. de Rosny, and S. Tretyakov, "Smart radio environments empowered by reconfigurable intelligent surfaces: How it works, state of research, and road ahead," *IEEE Journal on Selected Areas in Communications*, 2020.
- [2] A. Zappone, M. Di Renzo, and M. Debbah, "Wireless networks design in the era of deep learning: Model-based, AI-based, or both?" *IEEE Transactions on Communications*, vol. 67, no. 10, pp. 7331–7376, October 2019.
- [3] M. Di Renzo *et al.*, "Smart radio environments empowered by reconfigurable AI meta-surfaces: An idea whose time has come," *EURASIP Journal on Wireless Communications and Networking*, vol. 129, 2019.
- [4] C. Huang, S. Hu, G. C. Alexandropoulos, A. Zappone, C. Yuen, R. Zhang, M. Di Renzo, and M. Debbah, "Holographic MIMO surfaces for 6G wireless networks: Opportunities, challenges, and trends," *IEEE Wireless Communications Magazine*, vol. in press, 2020.
- [5] E. Basar, M. Di Renzo, J. de Rosny, M. Debbah, M. S. Alouini, and R. Zhang, "Wireless communications through reconfigurable intelligent surfaces," *IEEE Access*, vol. 7, pp. 116 753 – 116 773, 2019.
- [6] M. Di Renzo and *et al.*, "Reconfigurable intelligent surfaces vs. relaying: Differences, similarities, and performance comparison," *IEEE Open Journal of the Communications Society*, vol. 1, pp. 798 – 807, 2019.
- [7] X. Qian, M. Di Renzo, J. Liu, A. Kammoun, and M.-S. Alouini, "Beamforming through reconfigurable intelligent surfaces in single-user MIMO systems: SNR distribution and scaling laws in the presence of channel fading and phase noise," <https://arxiv.org/pdf/2005.07472.pdf>, 2020.
- [8] S. Zhou, W. Xu, K. Wang, M. Di Renzo, and M. Alouini, "Spectral and energy efficiency of IRS-assisted MISO communication with hardware impairments," *IEEE Wireless Communications Letters*, in press, 2020.
- [9] W. Tang, M. Z. Chen, X. Chen, J. Y. Dai, Y. Han, M. Di Renzo, Y. Zeng, S. Jin, Q. Cheng, and T. J. Cui, "Wireless communications with reconfigurable intelligent surface: Path loss modeling and experimental measurement," <https://arxiv.org/abs/1911.05326>, 2019.

- [10] W. Tang, X. Li, J. Y. Dai, S. Jin, Y. Zeng, Q. Cheng, and T. J. Cui, "Wireless communications with programmable metasurface: Transceiver design and experimental results," *China Communications*, vol. 16, no. 5, pp. 46–61, May 2019.
- [11] W. Tang, J. Y. Dai, M. Chen, X. Li, Q. Cheng, S. Jin, K.-K. Wong, and T. J. Cui, "Programmable metasurface-based RF chain-free 8PSK wireless transmitter," *IEEE Electronic Letters*, vol. 55, no. 7, pp. 417–420, 2019.
- [12] L. Dai *et al.*, "Reconfigurable intelligent surface-based wireless communication: Antenna design, prototyping and experimental results," *IEEE Access*, vol. 8, pp. 45 913 – 45 923, 2020.
- [13] C. Huang, A. Zappone, G. C. Alexandropoulos, M. Debbah, and C. Yuen, "Reconfigurable intelligent surfaces for energy efficiency in wireless communication," *IEEE Trans. on Wireless Commun.*, vol. 18, no. 8, pp. 4157–4170, 2019.
- [14] Q. Wu and R. Zhang, "Intelligent reflecting surface enhanced wireless network: Joint active and passive beamforming design," *IEEE Transactions on Wireless Communications*, vol. 18, no. 11, pp. 5394–5409, November 2019.
- [15] Y. Yang, S. Zhang, and R. Zhang, "IRS-enhanced OFDM: Power allocation and passive array optimization," *IEEE Wireless Communications Letters*, vol. 9, no. 6, pp. 760 – 764, 2020.
- [16] X. Yu, D. Xu, and R. Schober, "MISO wireless communication systems via intelligent reflecting surfaces," in *2019 IEEE/CIC International Conference on Communications in China (ICCC)*, 2019.
- [17] R. Liu, H. Li, M. Li, and Q. Liu, "Symbol-level precoding design for intelligent reflecting surface assisted multi-user MIMO systems," <https://arxiv.org/abs/1909.01015>, 2019.
- [18] T. Jiang and Y. Shi, "Over-the-air computation via intelligent reflecting surfaces," *2019 IEEE Global Communications Conference (GLOBECOM)*, 2019.
- [19] X. Li, J. Fang, F. Gao, and H. Li, "Joint active and passive beamforming for intelligent reflecting surface-assisted massive MIMO systems," <https://arxiv.org/abs/1912.00728>, 2019.
- [20] H. Han *et al.*, "Intelligent reflecting surface aided network: Power control for physical-layer broadcasting," <https://arxiv.org/abs/1910.14383>, 2019.
- [21] C. Pan, H. Ren, K. Wang, W. Xu, M. ElKashlan, A. Nallanathan, and L. Hanzo, "Multicell MIMO communications relying on intelligent reflecting surface," *IEEE Transactions on Wireless Communications*, in press, 2020.
- [22] P. Wang, J. Fang, X. Yuan, Z. D. Chen, H. Duan, and H. Li, "Intelligent reflecting surface-assisted millimeter wave communications: Joint active and passive precoding design," <https://arxiv.org/abs/1908.10734>, 2019.
- [23] C. You, B. Zheng, and R. Zhang, "Intelligent reflecting surface with discrete phase shifts: Channel estimation and passive beamforming," *IEEE Journal on Selected Areas in Communications*, in press, 2020.
- [24] C. Pan, H. Ren, K. Wang, M. ElKashlan, A. Nallanathan, J. Wang, and L. Hanzo, "Intelligent reflecting surface aided MIMO broadcasting for simultaneous wireless information and power transfer," *IEEE Journal on Selected Areas in Communications*, in press, 2020.
- [25] H. Han, J. Zhao, Z. Xiong, D. Niyato, M. Di Renzo, Q. V. Pham, and W. Lu, "Intelligent reconfigurable surface aided power control for physical-layer broadcasting," [arXiv preprint arXiv:1912.03468](https://arxiv.org/abs/1912.03468), 2020.
- [26] N. S. Perovi, M. Di Renzo, and M. F. Flanagan, "Channel capacity optimization using reconfigurable intelligent surfaces in indoor mmWave environments," [arXiv preprint arXiv:1910.14310](https://arxiv.org/abs/1910.14310), 2020.
- [27] A. Zappone, M. Di Renzo, F. Shams, X. Qian, and M. Debbah, "Overhead-aware design of reconfigurable intelligent surfaces in smart radio environments," <https://arxiv.org/abs/2003.02538>, 2020.
- [28] G. Zhou, C. Pan, H. Ren, K. Wang, and A. Nallanathan, "A framework of robust transmission design for IRS-aided MISO communications with imperfect cascaded channels," <https://arxiv.org/abs/2001.07054>, 2020.
- [29] S. Hong, C. Pan, H. Ren, K. Wang, K. Chai, and A. Nallanathan, "Robust transmission design for intelligent reflecting surface aided secure communication systems with imperfect cascaded CSI," <https://arxiv.org/abs/2004.11580>, 2020.
- [30] G. Zhou, C. Pan, H. Ren, K. Wang, M. Di Renzo, and A. Nallanathan, "Robust beamforming design for intelligent reflecting surface-aided MISO communication systems," *IEEE Wireless Communications Letters*, in press, 2020.
- [31] K. Miettinen, *Nonlinear Multiobjective Optimization*. Springer, 1999.